A new allosteric site in glycogen phosphorylase b as a target for drug interactions

Nikos G Oikonomakos[1]*, Vicky T Skamnaki[1], Katerina E Tsitsanou[1], Nikos G Gavalas[1] and Louise N Johnson[2]

Background: In muscle and liver, glycogen concentrations are regulated by the coordinated activities of glycogen phosphorylase (GP) and glycogen synthase. GP exists in two forms: the dephosphorylated low-activity form GPb and the phosphorylated high-activity form GPa. In both forms, allosteric effectors can promote equilibrium between a less active T state and a more active R state. GP is a possible target for drugs that aim to prevent unwanted glycogen breakdown and to stimulate glycogen synthesis in non-insulin-dependent diabetes. As a result of a data bank search, 5-chloro-1*H*-indole-2-carboxylic acid (1-(4-fluorobenzyl)-2-(4-hydroxypiperidin-1-yl)-2-oxoethyl)amide, CP320626, was identified as a potent inhibitor of human liver GP. Structural studies have been carried out in order to establish the mechanism of this unusual inhibitor.

Results: The structure of the cocrystallised GPb–CP320626 complex has been determined to 2.3 Å resolution. CP320626 binds at a site located at the subunit interface in the region of the central cavity of the dimeric structure. The site has not previously been observed to bind ligands and is some 15 Å from the AMP allosteric site and 33 Å from the catalytic site. The contacts between GPb and CP320626 comprise six hydrogen bonds and extensive van der Waals interactions that create a tight binding site in the T-state conformation of GPb. In the R-state conformation of GPa these interactions are significantly diminished.

Conclusions: CP320626 inhibits GPb by binding at a new allosteric site. Although over 30 Å from the catalytic site, the inhibitor exerts its effects by stabilising the T state at the expense of the R state and thereby shifting the allosteric equilibrium between the two states. The new allosteric binding site offers a further recognition site in the search for improved GP inhibitors.

Addresses: [1]Institute of Biological Research and Biotechnology, The National Hellenic Research Foundation, 48 Vassileos Constantinou Avenue, Athens 11635, Greece and [2]Laboratory of Molecular Biophysics, University of Oxford, South Parks Road, Oxford OX1 3QU, UK.

*Corresponding author.
E-mail: nikos@krokees.eie.gr

Key words: allosteric inhibition, diabetes, glycogen metabolism, glycogen phosphorylase, protein–drug interactions

Received: **8 February 2000**
Revisions requested: **16 March 2000**
Revisions received: **31 March 2000**
Accepted: **4 April 2000**

Published: **23 May 2000**

Structure 2000, **8**:575–584

0969-2126/00/$ – see front matter

Introduction

Non-insulin-dependent diabetes is characterised by elevated blood glucose levels that arise from resistance to the action of insulin and/or a deficiency in insulin secretion [1,2]. Insulin promotes the deposition of glycogen in the liver and triglyceride in adipose tissues, and also activates glucose transport and glycogen synthesis in muscle. Type 2 diabetes is treated with diet, exercise, drugs that promote insulin release from the β cells of the pancreas, and with insulin. Such treatment is not always satisfactory, especially in the control of extreme fluctuations in blood glucose levels, and there is a continued search for new compounds to treat this condition. Glycogen phosphorylase (GP; E.C.2.4.1.1) offers a potential target for such compounds because of its essential roles in glycogen metabolism and control of liver glucose output.

GP catalyses the degradative phosphorolysis of glycogen to glucose-1-phosphate (glucose-1-P). In muscle, glucose-1-P is utilised via glycolysis to generate metabolic energy, but in the liver it is mostly converted to glucose, which is output for the benefit of other tissues [3]. Both in muscle and liver, GP exists in two interconvertible forms: the dephosphorylated form (GPb, low activity and low substrate affinity) and the Ser14-phosphorylated form (GPa, high activity and high substrate affinity). With both forms, allosteric effectors can promote equilibrium between a less active T state and a more active R state, the structures of which have been characterised (reviewed in [4–6]). Insulin stimulates muscle and liver cells to transport glucose out of the blood stream and to store it within the cell in the form of glycogen. In the liver, glucose itself assists the process of switching the cell from glycogenolysis to glycogen synthesis. Glucose is a competitive inhibitor of GPa and thus decreases glycogenolysis [7]. It also promotes the less active T state of GPa, which is a better substrate than the R state for the inactivating enzyme protein phosphatase 1. GPa, but not GPb, is a potent inhibitor of the phosphatase

action on glycogen synthase and it is only when GP has been dephosphorylated that the phosphatase is free to activate glycogen synthase [8,9].

These observations led to the search for glucose analogue inhibitors that would promote the T state and allow modulation of glycogen metabolism. Crystallographic studies with the rabbit muscle enzyme (which is over 80% homologous to the liver isoform) showed highly specific binding of the glucose analogues at the catalytic site of GP and stabilisation of the T state conformation. These inhibitors were designed on the basis of information derived from the X-ray crystal structure of T state rabbit muscle GPb [10–15]. Compounds that were 1000 times more potent than glucose were found that achieved the desired effects in modulating GP activity in hepatic cells [16–18]. However, these compounds failed to stimulate glycogen synthase activity in cells because of modification by phosphorylation in the cell; the phosphorylated compounds failed to activate glycogen synthase [17,19]. Nevertheless, the rationale for targeting GP through modulating its allosteric properties has continued to be of interest. Compounds unrelated to the physiological regulators of GP can exert potent effects, for example, the compound Bay W1807 (K_i = 1.6 nM) regulates activity through recognition at the AMP-binding site [20].

Figure 1

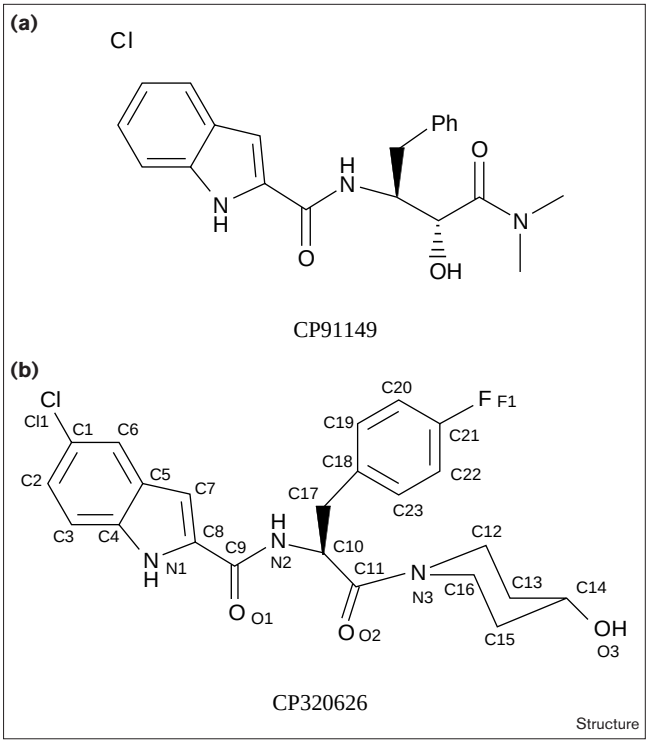

The chemical structures of **(a)** CP91149 and **(b)** CP320626, showing the numbering system used.

As part of a screening process to identify compounds that might contribute to the regulation of glycogen metabolism, CP91149 (Figure 1a) was discovered by high-throughput screening of >300,000 compounds, from a sample bank, against recombinant human liver GPa [21]. CP91149 was characterised *in vitro* and *in vivo* and shown to be an inhibitor of human liver GPa with an IC_{50} of 1 μM. The compound acts synergistically with both glucose (IC_{50} = 130 nM) and caffeine (IC_{50} = 140 nM) when measured in the direction of glycogen synthesis, suggesting that CP91149 is kinetically distinct from both glucose and caffeine. Two series of compounds derived from CP91149, 3-((indole-2-carbonyl)amino)-2-hydroxy-4-phenyl-butyric acid and *N*-(indole-2-carbonyl)phenylalanine analogues, were also synthesised and assessed for their ability to inhibit liver GPa and glycogenolysis [22]. The related compound CP320626 (Figure 1b), is a potent inhibitor of human liver GPa (IC_{50} = 205 nM in the presence of glucose) and has been shown to produce marked glucose lowering at 10 mg kg^{-1} in diabetic *ob/ob* mice, without altering plasma insulin levels [22].

GP contains at least five potential regulatory sites: the Ser14 phosphate-recognition site, the AMP activatory and the glucose-6-P inhibitory allosteric sites, the catalytic site that binds glycogen and glucose-1-P, the inhibitor site located 12 Å from the catalytic site which binds caffeine and related compounds, and the glycogen storage site. CP320626 has no apparent structural relation to any of the physiological compounds that bind to these sites. To investigate how this and related compounds bind to GP, we have determined the structure of the cocrystallised rabbit muscle GPb–CP320626 complex. The structure reveals a new allosteric site situated at the dimer interface that has not been previously identified. In order to compare the structural results obtained for the muscle enzyme with the kinetic results reported for the liver enzyme, we demonstrate through kinetic studies that CP320626 has a similar potency on rabbit muscle GP to that observed with the human liver and muscle isoforms.

Results and discussion

Effects of CP320626 on GPb activity

IC_{50} values for CP320626 inhibition of rabbit muscle GPb without or with 10 mM glucose were 334 ± 10 nM and 178 ± 10 nM, respectively. Hoover *et al.* [22] reported IC_{50} values of 205 nM and 83 nM for CP320626 inhibition of human liver GPa and human muscle GPa, respectively, in the presence of 0.5 mM glucose-1-P, 0.1% glycogen and 7.5 mM glucose, in a buffer consisting of 50 mM HEPES (pH 7.2), 100 mM KCl, 2.5 mM EDTA, 2.5 mM $MgCl_2$ at 22°C. The slightly different IC_{50} values might be due to the different isoforms and different substrate concentrations and assay conditions used. The relative potency of the inhibitor observed in our kinetic

Figure 2

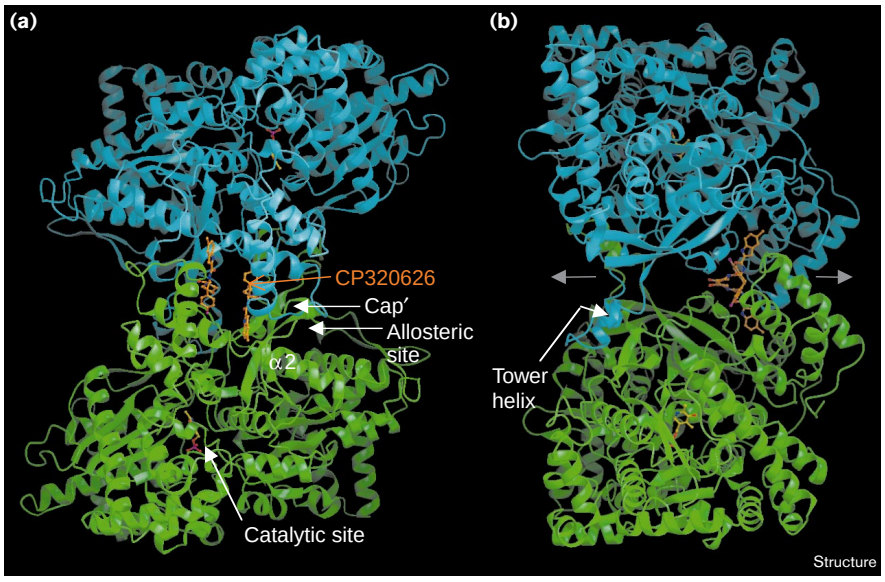

A schematic diagram of the GPb dimer with bound CP320626. One subunit is coloured green and the other cyan. CP320626 is shown in orange. **(a)** A view down the molecular dyad showing the positions for the catalytic site, allosteric effector site, and CP320626-binding site together with the α2 helix and the cap′ region from the other subunit. The catalytic site, marked by the essential cofactor pyridoxal 5′-phosphate, is buried at the centre of the subunit and is accessible to the bulk solvent through a 15 Å long channel that exits on the far side of the molecule. Access to the site for bulky ligands, such as glycogen, is blocked in the T state. The inhibitor site (not shown), which binds purine compounds such as caffeine, is situated at the entrance to the catalytic site tunnel. Occupation of this site stabilises the T-state conformation of the enzyme and blocks access to the catalytic site, thereby inhibiting the enzyme in synergism with glucose at the catalytic site. The allosteric site, which binds the activator AMP, the weak activator IMP and other phosphorylated compounds such as the allosteric inhibitor glucose-6-P, is situated at the subunit–subunit interface (between the α2 and α8 helices of one subunit and cap′ of the other subunit) some 30 Å from the catalytic site. The CP320626-binding site, located inside the central cavity between the two subunits, is some 15 Å from the allosteric effector site, 33 Å from the catalytic site and 37 Å from the inhibitor site. **(b)** A view, rotated 90° with respect to (a), normal to the twofold axis. The CP320626-binding site and the α2–cap′ interface are to the right and the tower–tower′ subunit–subunit interface to the left of the figure. The catalytic site is marked by pyridoxal phosphate at the centre of each subunit. Access to the catalytic site is via a channel to the left of the figure.

experiments (a factor of 1.9) without/with glucose is consistent with the synergy observed previously with CP911149 and glucose. Synergy with glucose confers an additional benefit, allowing the effector to modulate its effect in response to glucose concentrations.

CP320626-binding site

The overall architecture of the native T state GPb and the catalytic and the allosteric sites have been described previously [4] (Figure 2). The two subunits of the functionally active dimer are related by a crystallographic twofold symmetry axis and enclose a solvent-filled central cavity surrounded on each side by residues from the N-terminal domains of both subunits. The structure of the cocrystallised GPb–CP320626 complex has been refined at 2.3 Å to a crystallographic R value of 0.199 (R_{free} = 0.246) (Table 1). CP320626 binds in the central binding cavity between the two subunits; this is the first time a ligand has been reported to bind at this site. The binding site is some 15 Å from the AMP allosteric effector site, 33 Å from the catalytic site, and 37 Å from the caffeine inhibitor site.

The central cavity of T state GPb is ~30 Å long, with a radius that varies from a maximum of ~8 Å to a minimum of ~4 Å, and encloses a volume of 1300 Å^3. The cavity is partially closed at one end by residues from the cap and α2 helices (Arg33, His34, Arg60 and Asp61 and their symmetry-related equivalents) and at the other end by the tower helices (residues Asn270, Glu273, Ser276 and their symmetry-related equivalents; Figure 2). In the 2.0 Å resolution 100K T state GPb structure [15], 60 water molecules have been located in the cavity (30 water molecules from each subunit). These water molecules form few contacts with the protein: only four out of the 30 make more than one hydrogen bond to protein atoms. Nine water molecules present in the native T state GPb structure become displaced on binding CP320626, five from one subunit and four from the symmetry-related subunit.

The inhibitor becomes almost entirely buried on forming the complex with GPb. The solvent accessibilities of the free and bound CP320626 molecules are 643 Å^2 and 107 Å^2, indicating that a surface area of 536 Å^2, respectively, becomes inaccessible to water and that CP320626 becomes 83% buried in the enzyme complex. Binding of CP320626 is associated with both subunits and nearly equal surface areas from the two subunits are buried in the inhibitor complex (307 Å^2 from one subunit and 229 Å^2 from the other). Both polar and nonpolar groups are buried, but the greatest contribution comes from the nonpolar groups, which contribute 457 Å^2 (85%) of the surface that becomes inaccessible.

Table 1

Diffraction data and refinement statistics for the T-state GPb–CP320626 complex.

Space group	$P4_32_12$
Unit-cell dimensions	
a,b,c (Å)	129.2,129.2,116.2
No. of images (°)	32 (1°)#
Resolution range (Å)	30–2.3 Å
No. of observations	160,475
No. of unique reflections	42,617
I/σ(I) (outermost shell)*	6.8 (1.7)
Completeness (outermost shell) (%)	96.3 (91.0)
R_{merge} (outermost shell)†	0.110 (0.445)
Multiplicity	3.8
Outermost shell (Å)	2.34–2.30
Refinement (resolution) (Å)	30–2.3
No. of reflections used in refinement	40,437
No. of reflections used for R_{free}	2162
Residues included	13–842
No. of protein atoms	6749
No. of water molecules	256
No. of ligand atoms	
PLP	15
CP320626	32
Final R (R_{free}) (%)‡	19.9 (24.6)
Rmsd in bond lengths (Å)	0.008
Rmsd in bond angles (°)	1.4
Rmsd in dihedral angles (°)	25.6
Rmsd in improper angles (°)	0.7
Average B factor (Å²)	13–842
for protein residues	
overall	30.7 (27.1)§
CA,C,N,O	29.4 (25.8)§
sidechain atoms	32.0 (28.4)§
Average B (Å²) for ligands	
PLP	17.1
CP320626	19.8
water molecules	33.8

*σ(I) is the standard deviation of I. †$R_{merge} = \Sigma_t\Sigma_\eta \mid \langle I_h \rangle - I_{ih} \mid / \Sigma_t \Sigma_\eta I_{ih}$, where $\langle I_{ih} \rangle$ and ith are the mean and ith measurement of intensity for reflection h, respectively. ‡Crystallographic R factor = $\Sigma \mid \mid F_o \mid - \mid F_c \mid \mid / \Sigma \mid F_o \mid$, where $\mid F_o \mid$ and $\mid F_c \mid$ are the observed and calculated structure factor amplitudes, respectively. R_{free} is the corresponding R value for a randomly chosen 5% of the reflections that were not included in the refinement. § The average B factor (Å²) (given in parentheses) for protein residues if the poorly defined residues were excluded. #1° is the rotation range per image.

Interactions of CP320626 with protein residues

Views of the final electron-density map for the GPb–CP320626 complex are shown in Figure 3. The central C10 atom (with *S* stereochemistry) is tetrahedral and the planes of the 5-choro-1*H*-indole ring, the fluorophenylalanine ring and the 4-hydroxy-piperidyl ring are almost mutually perpendicular. One carbonyl group, the indolecarboxy carbonyl O1, is coplanar with the indole ring and the other carbonyl group, the piperidyl carbonyl O2, is approximately coplanar with the 4-hydroxy-piperidyl. There are no intramolecular hydrogen bonds. The 5-chloro-1*H*-indole ring binds to a pocket formed mostly by one subunit whereas the fluorophenylalanine ring binds to the walls of the central cavity and contacts the other subunit, as shown in Figure 4a.

The interactions of CP320626 with GPb involve six hydrogen bonds and 111 van der Waals contacts (within 4.0 Å), 47 of which are interactions between nonpolar groups (Figure 4b; Tables 2 and 3). The 1*H*-indole-2-carboxamide-binding pocket is formed by residues Arg60, Val64 and Trp67 of the α2 helix, the loop residues Pro188, Trp189 and Glu190, Lys191 at the start of the short β7 strand, Pro229 from strand β10 and Thr38′ and Val40′ of the cap′ region (where the prime refers to residues from the symmetry-related subunit). This part of the inhibitor exploits numerous van der Waals contacts that are dominated by the substantial contacts made to almost all atoms of Arg60. The sidechain of Arg60 stacks against the 1*H*-indole-2-carboxamide group making some 23 van der Waals contacts. The interaction of Arg60 on one side of the indole ring and Lys191 on the other side involve interactions characteristic of CH–π interactions [23] between the hydrogen atoms of the aliphatic carbons and the π electrons of the aromatic ring. The NE atom of the arginine is 3.4 Å from the ring centre of the indole and there is scope for amino–aromatic interactions, as observed in several protein–ligand complexes [24] including complexes between the phosphotyrosine-recognition domain SH2 and phosphotyrosine peptides [25]. The chlorine of the indole ring is buried in a pocket where it makes van der Waals interactions to Arg60, Val64 and Trp67 from adjacent turns of the α2 helix. There are hydrogen bonds from N1 of the indole ring to the mainchain oxygen atom of Glu190, from the N2 of the carboxamide to the mainchain oxygen of Thr38′ and a water-mediated hydrogen bond from the carbonyl O1 to the mainchain nitrogen of Ala192.

The 4-fluorobenzyl (or the fluorophenylalanine) moiety makes 47 van der Waals contacts (20 nonpolar–nonpolar) to residues that are all from the symmetry-related subunit. The 4-fluorobenzyl and Phe53′ rings are inclined approximately 60° and there are extensive contacts between them (Table 3). These contacts are augmented by nonpolar contacts to the edge of His57′ and to residues Thr38′, Leu39′ and Pro188′. The fluorine atom makes 15 van der Waals contacts and there are two polar contacts between the fluorine atom and residues 187′ and 188′, a short contact with the mainchain nitrogen atom of Pro188′ (2.8 Å) and a longer contact with the mainchain nitrogen of Asn187′ (3.3 Å).

The 4-hydroxy-piperidyl moiety makes relatively few van der Waals interactions with the protein and 11 out of 14 contacts are to water molecules in the central cavity. There are three hydrogen bonds: a direct hydrogen bond from piperidyl carbonyl O2 to Lys191 (NZ) and water-mediated hydrogen bonds from the piperidyl N3 to Ala192 (N) and from the 4-hydroxy-piperidyl O3 to the OH of Tyr226.

Figure 3

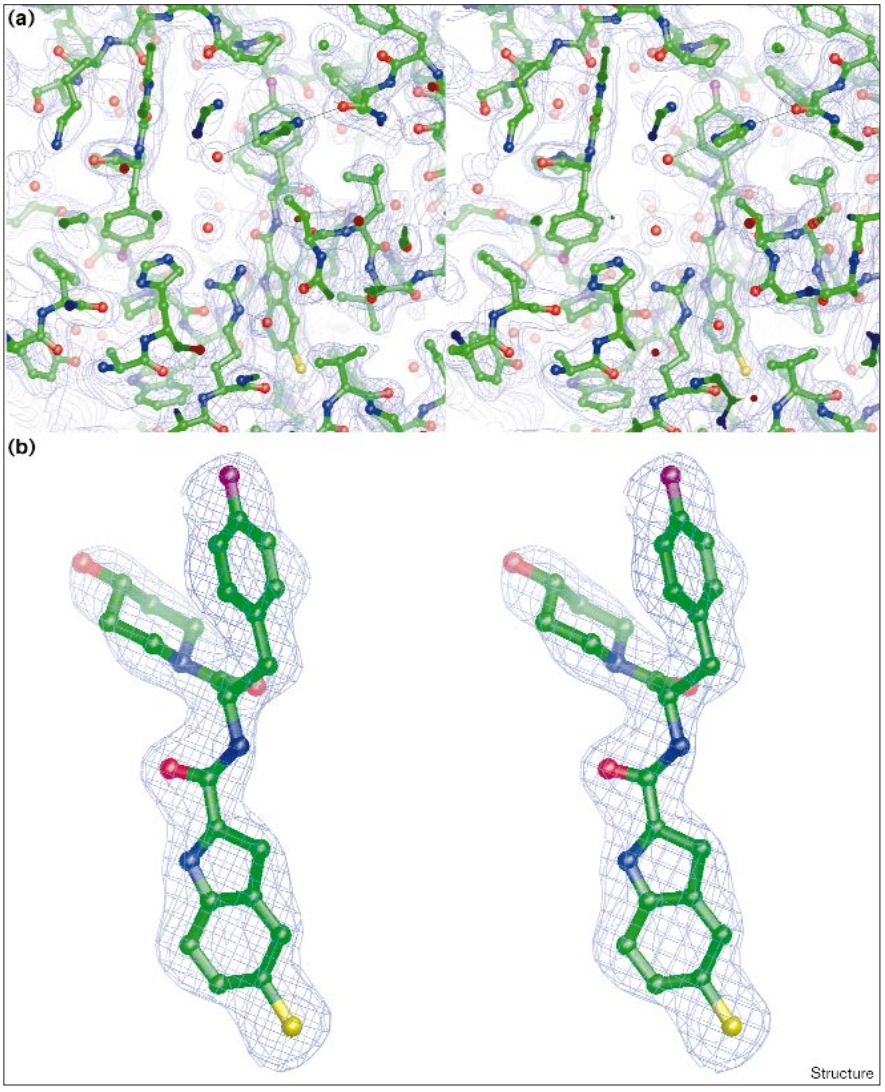

Stereo diagrams of the electron density of the final weighted $2F_o–F_c$ map. **(a)** The CP320626-binding site. **(b)** A close up of the bound CP320626 molecule. The contour level corresponds to approximately 1 root mean square deviation calculated for the map.

The 18 amino acid residues (nine from each subunit) implicated in CP320626 binding are highly conserved in GPs from human muscle, human liver, human brain, rat muscle, rat liver and rat brain [26]. With the exception of Ala192 (which is serine in the human liver isoenzyme), a total of 17 residues that come into close contact with CP320626 are identical in the rabbit muscle and human liver GPs. This suggests that the site is likely to be the same in the liver enzyme.

Conformational changes

There are negligible changes in the mainchain conformation on binding of CP32026 to GPb, but there are shifts in some residues surrounding the inhibitor. The superposition of the structures of the native T state GPb and the GPb–CP320626 complex over the well-defined residues (16–208, 213–249, 261–313, 326–549 and 558–830) gave root mean square (rms) deviations of 0.138, 0.151 and 0.351 Å for Cα, mainchain and sidechain atoms, respectively, indicating that the two structures have very similar overall conformations to within the limits of the resolution of the study. The greatest changes involve shifts of the sidechain of Arg60. In the native GPb structure, Arg60 restricts the 5-choro-1*H*-indole pocket, but in the GPb–CP320626 complex this residue shifts by ~1.3–3.5 Å in order to optimise binding. There are also shifts of the sidechain atoms of Val64 by ~2.0–2.2 Å, and shifts of the sidechain atoms of Lys191 of ~0.6–1.3 Å that improve contacts with the chlorine atom and the 4-hydroxy-piperidyl group, respectively. There are no changes at the catalytic site, at the inhibitor site or at the tower–tower′ helix subunit interface.

In the native T state GPb structure, there are hydrogen bonds across the subunit interface in the vicinity of the

Figure 4

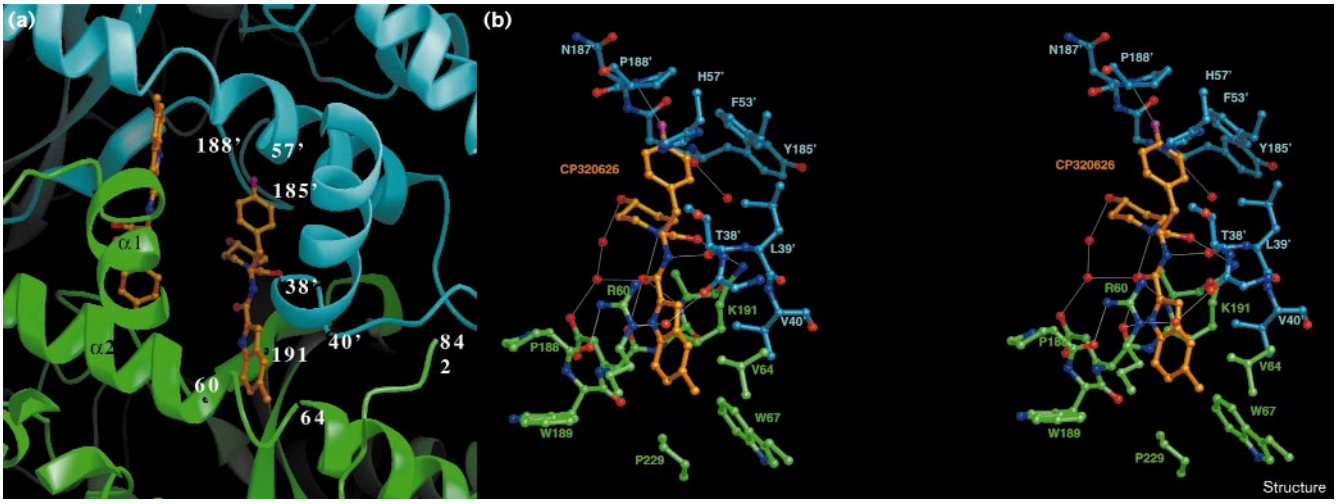

Details of the CP320626-binding site. **(a)** Close-up view of the central cavity showing the CP320626 allosteric binding site in the same orientation and colour scheme as Figure 2a. The Cα positions of certain key residues mentioned in the text are labeled (Arg60, Val64, Lys191, Thr38′, Val40′, His57′, Tyr185′ and Pro188′). The C-terminal tail, with the C-terminal residue 842 labeled, is visible in the lower right. The shortest and longest distances between the two symmetry-related CP320626 molecules when bound to GPb are 5.6 Å (C13–C13′) and 12.8 Å (O2–O2′), respectively. **(b)** Details of the interactions between CP320626 and GPb shown in stereo. The chloroindole-binding pocket is in the lower part of the figure and the fluorophenylalanine-binding pocket in the upper part. The view is the same as in (a). Hydrogen bonds are shown as thin lines.

CP320626-binding site that are important for maintaining the dimer structure [27]. Arg60 hydrogen bonds to the mainchain oxygen of Phe37′ (2.9 Å), Arg193 hydrogen bonds to the mainchain oxygens of residues Leu39′ (2.9 Å) and Val40′ (2.9 Å) and Glu195 hydrogen bonds to Lys41′ (2.9 Å). On forming the complex with CP320626, the major shift in Arg60 and the minor shifts in residues 39′–40′ cause the intersubunit hydrogen bond between Arg60 and Phe37′ to be broken. However, the intersubunit hydrogen-bonding pattern between residues 193 and 195 and residues 39′ and 40′ is not significantly changed. The hydrogen bonds of Arg193 to the mainchain oxygen of Leu39′ (3.4 Å) and Val40′ (3.4 Å) are weakened, but Glu195 is still able to hydrogen bond to Lys41′ (2.9 Å). The Tyr185′–Pro194 contact, which is an important subunit–subunit contact and a major link between the cap′–α2 helix and the tower–tower′contacts [28], is also retained in the GPb–CP320626 complex.

Table 2

Hydrogen bonds* between CP320626 and GPb.

Inhibitor atom	Protein atom	Distance (Å)
N1	Glu190 O	2.9
O1	Wat159	3.2
N2	Thr38′ O	2.9
O2	Lys191 NZ	2.9
N3	Wat159	3.0
O3	Wat92	3.0

*Hydrogen-bonds were assigned if the distance between the electronegative atoms was less than 3.3 Å and if both angles between these atoms and the preceding atoms were greater than 90°. Wat92 is hydrogen bonded to Tyr226 OH (3.1 Å) and to Wat158 (3.2 Å); Wat158 is in turn hydrogen bonded to Glu190 OE1 (2.8 Å); Wat159 is hydrogen bonded to Ala192 N (2.5 Å) and to Wat158 (2.9 Å).

Comparison with GPa in the R state

Liver GP is controlled mostly by the phosphorylation/dephosphorylation of Ser14 and is much less responsive than the muscle enzyme to allosteric effectors such as AMP [3]. Modelling studies on the liver isoform suggest that the two enzymes, which are 80% identical in sequence, are likely to have very similar structures, although there may be some differences at the tower–tower′ subunit interface [16]. These differences do not affect the CP320626-binding site as discussed above. It is, therefore, of interest to compare the CP320626-binding site in GPb and GPa as this might help us to understand the basis for inhibition and synergy with glucose.

The conversion of the less active T state muscle GPb to the active R state GPa involves changes in the tertiary and quaternary structure [29–32]. In the R state, relative to the T state, one subunit is rotated relative to the other by 9.6° so as to bring the two subunits closer together at the α2′–cap interface and causing them to move further apart at the tower–tower′ interface of the dimer. The contacts at the α2–cap′ interface are increased either by the contacts to the Ser14 phosphate or by contacts to the allosteric

effector AMP. The movements at the tower–tower′ interface lead to displacement of a loop (the 280s loop) that blocks the access of large ligands such as glycogen to the catalytic site. Displacement of this loop removes an acidic residue (Asp283) from proximity with the 5′-phosphate of the cofactor pyridoxal phosphate and allows replacement of the acidic residue by a basic residue (Arg569) that creates an anion recognition site for the phosphate substrate. Thus changes at the subunit interfaces are closely coupled to changes at the catalytic site.

Comparison of the T state GPb–CP320626 complex with R state GPa [31] shows that the ligand-binding site is likely to have considerably lower affinity in GPa. Superposition of the structure of the R state GPa (subunit A) with the structure of the GPb–CP320626 complex gave rms deviations of 1.201, 1.213 and 2.028 Å for Cα, main-chain and sidechain atoms, respectively, for ordered residues 16–208, 213–249, 261–313, 326–549 and 558–830. In GPa the CP320626-binding site is squeezed at the 5-chloro-1*H*-indole pocket and is more open at the fluorophenylalanine site as a consequence of these changes in tertiary and quaternary structure (Figure 5). The conformational changes in the α2 helix lead to a more perfect α helix in GPa and the Cα atoms of Arg60 and Val64 are 0.7 Å closer in GPa than in GPb (Figure 5a). The sidechains of residues Arg60 and Lys191 would be required to move in order to open up the site, as indeed they do on forming the GPb–CP320626 complex, but the close contact between the sidechain of Val64 and CP320626 would be difficult to relieve when the α2 helix is locked in the R-state conformation. At the fluorophenylalanine site, the shift in the symmetry-related subunit by ~2 Å results in the loss of contacts to Phe53′ and Tyr185′ (Figure 5b). The changed shape of the cavity between GPb and GPa shows that the T-state conformation favours binding of CP320626 whereas the R state does not. Conversely, binding of CP320626 will shift the equilibrium between the R and T states in favour of T state.

Potency and selectivity

The structure of the GPb–CP320626 complex pinpoints specific interactions responsible for the high affinity and selectivity of CP320626 for the enzyme. On binding to GPb, CP320626 exploits numerous van der Waals contacts that are dominated by the substantial nonpolar contacts to the aliphatic parts of Arg60 and Lys191, to Val64, to the edge atoms of Trp67 and Pro229, and to Thr38′, Leu39′, Val40′, Phe53′, His57′ and Pro188′ from the symmetry-related subunit (Figure 4; Table 3). These contacts comprise aromatic–aromatic interactions (4-fluorobenzyl group–Phe53′ sidechain), amino–aromatic interactions (His57′–4-fluorobenzyl group; Arg60–indole ring), CH–π electron interactions (Arg60 sidechain–indole ring; CE3 and CZ3 of Trp67–indole ring; CG and CD of Pro229–indole ring; Val40′ sidechain–indole ring; CA, CB and CD of Pro188′–4-fluorobenzyl group), and nonpolar–nonpolar interactions (CB of Ala192–C15 of the piperidyl group; CG2 of Thr38′–C17; and CD1 of Leu39′–C17). All of the polar groups on CP320626 are involved in hydrogen bonds either directly with the protein or through water molecules. The increase in entropy from the release of nine water molecules at the binding site, together with the van der Waals, CH–π, halogen–polar, and the specific polar–polar interactions appear to be the major source of binding energy that results in an inhibitor with high affinity for GPb. The contacts between GPb and CP320626 are remarkable because the enzyme has no biological reason to recognise this ligand.

Kinetic experiments [22] show that the 1*H*-indole-2-carboxamide moiety is an important determinant of selectivity in the two series of inhibitors derived from 3-((indole-2-carbonyl)amino)-2-hydroxy-4-phenyl-butyric acid and *N*-(indole-2-carbonyl)phenylalanine. The 1*H*-indole-2-carboxamide group binds in a pocket filled

Table 3

Van der Waals contacts* between CP320626 and GPb.

Inhibitor atom	Protein atom	No. of contacts
CL1	Arg60 O, CG; Val64 N, CA, CB; Trp67 CE3	6
C1	Arg60 CG, NE, CD; Trp67 CE3, CZ3; Val40′ CG2	6
C2	Arg60 CG, CD; Trp67 CZ3; Pro229 CG, CD	5
C3	Arg60 CD; Pro188 O; Trp189 O, C	4
C4	Arg60 NE, CD, CZ; Pro188 O; Glu190 O; Lys191 CB	6
N1	Arg60 CZ; Pro188 O; Glu190 C; Lys191 N, CA, CB	6
C5	Arg60 NE, CD, CZ, NH1; Val40′ CG2	5
C6	Arg60 CG, NE, CD; Val40′ CG2; Wat248	5
C7	Arg60 NE, CZ, NH1; Thr38′ O; Val40′ CG2	5
C8	Arg60 CZ, NH1; Glu190 O; Lys191 CD	4
C9	Thr38′ O	1
O1	Glu190 O	1
C10	Thr38′ O	1
C11	Wat159	1
O2	Lys191 CD, CE	2
C12	Wat159	1
C13	Wat158; Wat159	2
C14	Gly186′ CA; Wat92	2
O3	Gly186′ CA	1
C15	Ala192 CB; Tyr185′ O; Wat159; Wat247	4
C16	Wat159; Wat247	2
C17	Thr38′ O, CG2; Leu39′ CD1	3
C18	His57′ CE1, NE2	2
C19	His57′ CE1, NE2; Wat223′	3
C20	His57′ CE1, NE2; Pro188′ CA,CB	4
C21	Phe53′ CD2, CE2; His57′ CE1; Pro188′ N, CA, CB, CD	7
F1	Phe53′ CD2, CE2, CZ; Gly186′ O, C, CA; Asn187′ O, N, C, CA; Pro188′ CA, CB, N, CG, CD	15
C22	Phe53′ CG, CD2, CE2,CZ; His57′ CE1	5
C23	Leu39′ CD1; His57′ CE1	2
Total		111

*Van der Waals interactions were assigned for non-hydrogen atoms separated by less than 4 Å.

Figure 5

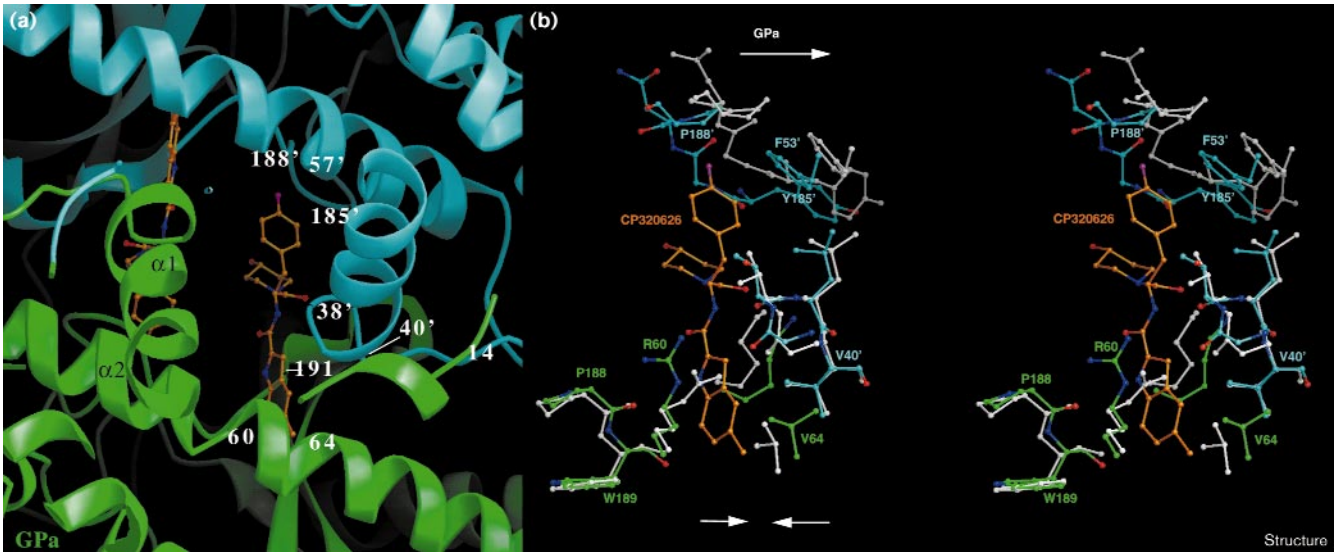

GPa in the R state viewed in a similar orientation to that of the GPb–CP320626 complex in Figures 2 and 4; the position of CP320626 is superimposed. **(a)** Close-up view of the CP320626 site in GPa with the Cα positions of residues shown in Figure 4a labeled. In R state GPa, the N-terminal tail containing the Ser14 phosphate group (lower right) displaces the C-terminal tail of GPb. The α2 helix adopts a more perfect helix in GPa compared with GPb and residues 60 and 64 are 0.7 Å closer together, thus squeezing the chloroindole-binding site. As a result of quaternary and tertiary structural changes, the loop comprising residues 185′–188′ and the α2′ helix from the other subunit shift ~2 Å so that the fluorophenylalanine site is more open. **(b)** Details of the CP320626 site in GPb, as in Figure 4b, with residues from GPa superimposed and shown in white. Some residues shown in Figure 4b have been omitted for clarity. The shifts in Arg60, Val64 and Lys191 in GPa block the chloroindole site as indicated by the two white convergent arrows. The shifts in residues 185′–188′ and Phe53′ (shown by the white arrow at the top) result in an open site at the fluorophenylalanine-binding site in GPa.

by close-packed sidechains and opening of this pocket requires a conformational change, mainly at the level of the sidechain of Arg60. The structure-activity relationships showed that changing the indole-5-substituent in the phenylalanine series reduced inhibitory activity in the order Cl ~ Br > F ~ H >OCH_3. Our structural results suggest that the Cl substituent does not fully occupy the space available and that there is enough space to accommodate Br, whereas substitution of the indole-5 with OCH_3 would result in a steric clash of the inhibitor with protein residues. Hydrogen bonding between N1 (-NH) of the indole ring and the mainchain oxygen of Glu190 appears to be important in enhancing the affinity of CP320626 for the enzyme. Substitution of N1 of the indole ring with N-CH_3, in N-methylindole, or with oxygen, in benzofuran, affects ligand affinity. Thus, for both compounds, the IC_{50} increases from 205 nM (with respect to human liver GPa) to >10,000 nM [22]. These differences in the IC_{50} values can be attributed to the lack of a hydrogen bond between the N1 atom and mainchain oxygen of Glu190 in the latter derivatives.

Mechanism of inhibition

The structural results show that the CP320626-binding site in GPb provides a bridge between the subunits. Although the small conformational changes in tertiary structure on forming the complex result in the loss of one hydrogen bond from Arg60 to the other subunit, the extensive nonpolar contacts and the six hydrogen bonds from the inhibitor to the protein strengthen the subunit–subunit interface and lock it in a conformation close to the T-state quaternary conformation. Thus, CP320626 acts as an allosteric inhibitor binding at a site distant from the catalytic site and exerting its effects by promoting the T-state conformation, consistent with the Monod–Wyman–Changeux [33] model for allosteric effects. Glucose binds more tightly to T-state GP making contacts to the 280s loop in the closed T-state conformation at the catalytic site. Therefore, by promoting the T state, CP320626 will also promote synergistic glucose binding. The CP320626 site is remote from both the AMP and Ser14 phosphate binding sites but all three sites make contacts to residues in two key regions of the protein — the α2 helix and the cap′ region of the other subunit. By tuning these contacts, effectors may promote either the T state or the R state. The result is reminiscent of that observed for the four novel potent allosteric inhibitors of hemoglobin: bezafibrate, LR16, L35, L345 and related compounds [34,35]. The binding sites of these inhibitors lie in the central water cavity, mainly between the α chains; the sites are distant from the allosteric 2,3-bisphosphoglycerate-binding site.

Biological implications

Type 2 diabetes is a prevalent disease that affects about 4–5% of the population. There is a continued search for compounds that can improve therapy. Liver glycogen phosphorylase (GP) has been identified as a possible target for drugs that control blood glucose concentrations. There are two forms of GP: the phosphorylated form (GPa) and the dephosphorylated form (GPb). In both forms, allosteric effectors can promote equilibrium between a less active T state and a more active R state.

A data bank search led to the identification of the compound 5-chloro-1*H*-indole-2-carboxylic acid (1-(4-fluorobenzyl)-2-(4-hydroxypiperidin-1-yl)-2-oxoethyl)amide (CP320626) as a potent inhibitor of GP. CP320626 shows no structural similarity to any natural regulators of phosphorylase activity. The crystallographic binding studies reported here with T state rabbit muscle GPb show that CP320626 occupies a buried site in the central cavity of the dimeric enzyme. The inhibitor makes extensive contacts between residues from both subunits and all but one of these residues are conserved in human liver GP, indicating that this site is the probable site of action in the liver enzyme. The contacts between CP320626 strengthen the subunit–subunit interface of the T-state conformation. The tertiary and quaternary structural changes that occur between the T-state and R-state phosphorylase result in subtle but significant changes at this subunit–subunit interface and a less favourable binding site in the R state. The structure highlights the importance of protein–protein interface interactions in oligomeric allosteric proteins. By binding at a site remote from the catalytic site and other effector sites, CP320626 is nevertheless able to influence catalytic activity by promoting the less active T-state conformation over the active R-state conformation. The structure reveals a new allosteric binding site for modulating activity that might prove of practical importance in the structure-based design of new inhibitors with improved pharmacological properties.

Materials and methods

Kinetic experiments

Rabbit muscle GPb was isolated, purified, freed of AMP and assayed as described [36] with minor modifications. The enzyme (5 μg ml^{-1}) was assayed at pH 6.8 and 30°C with 10 mM glucose-1-P, 1% glycogen and 1 mM AMP in 50 mM triethanolamine hydrochloride, 100 mM KCl, 1 mM EDTA, 1 mM DTT buffer, and 1% DMSO. The enzyme was preincubated with glycogen and a range of concentrations of CP320626 for 60 min at 30°C before the reaction was started by adding glucose-1-P. CP320626 was synthesised by MercaChem (Nijmegen, The Netherlands), according to the procedures described by Hoover *et al.* [22].

Crystallisation and data collection

The GPb–CP320626 complex was cocrystallised under conditions similar to those described previously [20]. Just before data collection, the crystals were transferred to a fresh buffer solution (3 mM DTT, 10 mM BES, 0.1 mM EDTA, 0.02% sodium azide, pH 6.7). There were only small changes in unit-cell dimensions on complex formation, resulting in volume changes of 1.0% compared with native crystals [27]. Data were collected from a single crystal using a rotating anode source ($\lambda = 1.5418$ Å) and an 18 cm small Mar detector. Crystal orientation, integration of intensities and data reduction were performed using DENZO and SCALEPACK [37].

Structure refinement

Crystallographic refinement of the GPb–CP320626 complex was performed with X-PLOR version 3.8 [38] using bulk-solvent corrections. All data between 30.0 and 2.3 Å were included with no sigma cut-off. The starting protein structure was the refined model of the room temperature GPb–glucose complex [39], with water molecules removed. The Fourier maps calculated with SIGMAA-weighted [40] ($2mF_o–DF_c$) and ($F_o–F_c$) coefficients indicated tight binding of CP320626 at a site not previously characterised and located in the region of the central cavity of the dimer. A model of CP320626 generated using the program SYBYL [41] was fitted to the electron-density map after torsion angles of the computed model were adjusted. Map interpretation was performed using the program O [42]. Several sidechains of the enzyme model were adjusted and water molecules were added to the atomic model and retained only if they met stereochemical requirements by using WATERPICK (in X-PLOR). The final model was refined by the conventional positional and restrained individual B-factor refinement protocol in X-PLOR to give a final R factor value of 19.9% ($R_{free} = 24.6\%$). The structure contained residues 13–842 and 256 water molecules. A Luzatti plot [43] determined using the X-PLOR protocol suggests an average positional error of ~0.25 Å. Residues where B-factor values of mainchain atoms exceed 60 $Å^2$ include 13–15 (71.8 $Å^2$), 209–212 (67.1 $Å^2$), 250–260 (91.4 $Å^2$), 314–325 (90.6 $Å^2$), 550–557 (76.0 $Å^2$) and 831–842 (87.1 $Å^2$). The same regions are also poorly ordered in the native enzyme structure. The model displays good stereochemistry as determined by PROCHECK [44] with 86.3% of residues in the most favoured regions, 10.6% in the additional allowed regions, 2.3% in the generously allowed regions and 0.8% of residues (Val259, Ser314, Arg319, Arg323, His556 and Lys840 of the most disordered regions of the protein) in the disallowed regions. A summary of the data processing statistics and refinement parameters for the GPb–CP320626 complex structure is given in Table 1. Volumes were calculated with the program VOIDOO [45] and solvent accessibilities were calculated with the program NACCESS [46].

Structure comparisons

GP structures were superimposed over well-defined residues using LSQKAB [47] and subunit rotations were determined following the method of Sprang *et al.* [32]. Structural units (N-domain core, C-domain core and activation locus) were those defined previously. The major shifts between the GPb–CP320626 complex and native GPb for Cα atoms are for residues 38′ to 46′ of the symmetry-related subunit (between 0.4–0.6 Å) from the cap′ region, residues 47′ to 75′ (between 0.5–0.8 Å) from the α2 helix, and residues 184′ to 196′ (between 0.4–0.6 Å) from the loop following the β6 strand and from the short strand β7. These shifts affect the subunit–subunit interface in the region between the cap′, α2 helix and the loop between strands β7 and β8 of the symmetry-related subunit. Coordinate sets used for the comparison were: T state GPb [27] (Protein Data Bank [PDB] ID code 1gpb), T state GPb–glucose complex [39] (ID code 2gpb), T state 100K GPb [15] (ID code 2gpn), R state GPa [31] (ID code 1gpa), and PLPP–GPb–AMP [32] (ID code 1pyg). Figures 2–5 were produced using XOBJECTS, a molecular illustration program (MEM Noble, unpublished results).

Accession numbers

The coordinates for the T state GPb–CP320626 complex have been deposited with the PDB, Brookhaven National Laboratory, Upton, NY 11973 (accession code 1C50).

Acknowledgements

This work was supported by a Wellcome Trust Biomedical Research Collaboration Grant to LNJ and NGO, the ESEP program of the Royal Society

of London with the National Hellenic Research Foundation, and the Greek Secretariat for Research and Technology (GSRT) PENED99 99ED237. We wish to acknowledge the assistance of Minakshi Ghosh and Elspeth Garman at the Laboratory of Molecular Biophysics, University of Oxford, Oxford, UK, for providing excellent facilities for data collection, and Spyros Zographos for help in the production of figures.

References

1. DeFronzo, R.A. (1988). The triumvirate: beta cell, muscle, liver; a collusion responsible for NIDDM. *Diabetes* **37**, 667-687.
2. Taylor, S.I. (1999). Deconstructing Type 2 diabetes. *Cell* **97**, 9-12.
3. Newgard, C.B., Hwang, P.K. & Fletterick, R.J. (1989). The family of glycogen phosphorylases: structure and function. *CRC Crit. Rev. Biochem. Mol. Biol.* **24**, 69-99.
4. Johnson, L.N., *et al.*, & Barford, D. (1989). Glycogen phosphorylase b. In *Allosteric Enzymes*. (Herve, G., ed.), pp. 81-127, CRC Press, Boca Raton, FL.
5. Johnson, L.N. (1992). Glycogen phosphorylase: control by phosphorylation and allosteric effectors. *FASEB J.* **6**, 2274-2282.
6. Oikonomakos, N.G., Acharya, K.R. & Johnson, L.N. (1992). Rabbit muscle glycogen phosphorylase b: structural basis of activation and catalysis. In *Post-translational Modification of Proteins*. (Harding, J.J. & Crabbe, M.J.C. eds), pp. 81-151, CRC Press, Boca Raton, FL.
7. Hers, H.G. (1976). The control of glycogen metabolism in the liver. *Annu. Rev. Biochem.* **45**, 167-189.
8. Cohen, P. (1989). The structure and regulation of protein phosphatases. *Annu. Rev. Biochem.* **58**, 453-508.
9. Bollen, M. & Stalmans, W. (1992). The structure, role and regulation of Type I protein phosphatases. *Crit. Rev. Biochem. Mol. Biol.* **27**, 227-281.
10. Martin, J.L., *et al.*, & Tsitura, H.S. (1991). Glucose analogue inhibitors of glycogen phosphorylase: the design of potential drugs for diabetes. *Biochemistry* **30**, 10101-10116.
11. Watson, K.A., *et al.*, & Johnson, L.N. (1994). Design of inhibitors of glycogen phosphorylase: a study of α- and β-C-glucosides and 1-thio-β-D-glucose compounds. *Biochemistry* **33**, 5745-5758.
12. Bichard, C.J.F., *et al.*, & Fleet, G.W.J. (1995). Potent inhibition of glycogen phosphorylase by a spirohydantoin of glucopyranose: first pyranose analogues of hydantocidin. *Tetrahedron Letts.* **36**, 2145-2148.
13. Oikonomakos, N.G., *et al.*, & Acharya, K.R. (1995). *N*-Acetyl-β-D-glucopyranosylamine: a potent T-state inhibitor of glycogen phosphorylase. *Protein Sci.* **4**, 2469-2477.
14. Watson, K.A., *et al.*, & Zographos, S.E. (1995). Glucose analogue inhibitors of glycogen phosphorylase: from crystallographic analysis to drug design using GRID-force field and GOLPE variable selection. *Acta Crystallogr. D* **51**, 458-472.
15. Gregoriou, M., *et al.*, & Johnson, L.N. (1998). The structure of a glycogen phosphorylase glucopyranose spirohydantoin complex at 1.8 Å resolution and 100K: the role of the water structure and its contribution to binding. *Protein Sci.* **7**, 915-927.
16. Board, M., Hadwen, M. & Johnson, L.N. (1995). Effects of novel analogues of D-glucose on glycogen phosphorylase activities in crude extracts of liver and skeletal muscle. *Eur. J. Biochem.* **228**, 753-761.
17. Board, M., Bollen, M., Stalmans, W., Kim, Y., Fleet, G.W.J. & Johnson, L.N. (1995). Effects of a C1 substituted glucose analogue on the activation states of glycogen synthase and glycogen phosphorylase in rat hepatocytes. *Biochem J.* **311**, 845-852.
18. Board, M. & Johnson, L.N. (1995). Effects of *N*-acetyl-β-D-glucopyranosylamine on glycogen metabolism by isolated hepatocytes. *Diabetes Res.* **28**, 95-109.
19. Board, M. (1997). *N*-Acetyl-β-D-glucopyranosylamine 6-phosphate is a specific inhibitor of glycogen-bound protein phosphatase 1. *Biochem. J.* **328**, 695-700.
20. Zographos, S.E., *et al.*, Johnson, L.N. (1997). The structure of glycogen phosphorylase b with an alkyl-dihydropyridine-dicarboxylic acid compound, a novel and potent inhibitor. *Structure* **5**, 1413-1425.
21. Martin, W.H., *et al.*, & Treadway, J.L. (1998). Discovery of a human liver glycogen phosphorylase inhibitor that lowers blood glucose *in vitro*. *Proc. Natl Acad. Sci. USA* **95**, 1776-1781.
22. Hoover, D.J., *et al.*, & Treadway, J.L. (1998). Indole-2-carboxamide inhibitors of human liver glycogen phosphorylase. *J. Med. Chem.* **41**, 2934-2938.
23. Nishio, M., Umezawa, Y., Hirota, M. & Takeuchi, Y. (1995). The CH/π interaction significance in molecular recognition. *Tetrahedron* **51**, 8665-8701.
24. Burley, S.K. & Petsko, G.A. (1988). Weakly polar interactions in proteins. *Adv. Protein Chem.* **39**, 125-189.
25. Waksman, G., *et al.*, & Kuriyan, J. (1992). Crystal structure of the phosphotyrosine recognition domain SH2 of v-src complexed with tyrosine-phosphorylated peptides. *Nature* **358**, 646-653.
26. Hudson, J.W., Golding, G.B. & Crerar, M.M. (1993). Evolution of allosteric control in glycogen phosphorylase. *J. Mol. Biol.* **234**, 700-721.
27. Acharya, K.R., Stuart, D.I., Varvill, K.M. & Johnson, L.N (1991). *Glycogen Phosphorylase: Description of the Protein Structure*. p123, World Scientific, London & Singapore.
28. Johnson, L.N., Snape, P., Martin, J.L., Acharya, K.R., Barford, D. & Oikonomakos, N.G. (1993). Crystallographic binding studies on the allosteric inhibitor glucose-6-phosphate to T state glycogen phosphorylase b. *J. Mol. Biol.* **232**, 253-267.
29. Sprang, S.R., *et al.*, & Johnson, L.N. (1988). Structural changes in glycogen phosphorylase induced by phosphorylation. *Nature* **336**, 215-221.
30. Barford, D. & Johnson, L.N. (1989). The allosteric transition of glycogen phosphorylase. *Nature* **340**, 609-614.
31. Barford, D., Hu, S.-H. & Johnson, L.N. (1991). The structural mechanism for glycogen phosphorylase control by phosphorylation and by AMP. *J. Mol. Biol.* **218**, 233-260.
32. Sprang, S.R., Withers, S.G., Goldsmith, E.J., Fletterick, R.J. & Madsen, N.B. (1991). The structural basis for the association of phosphorylase b with AMP. *Science* **254**, 1367-1371.
33. Monod, J., Wyman, J. & Changeux, J.-P. (1965). On the nature of allosteric transitions: a plausible model. *J. Mol. Biol.* **12**, 88-118.
34. Abraham, D.J., *et al.*, & Kumert, M.P. (1992). Allosteric modifiers of hemoglobin: 2-(4-(((3,5-disubstituted anilino)carbonyl)methyl)phenoxy)-2-methylproprionic acid derivatives that lower the oxygen affinity of hemoglobin in red cell suspensions, in whole blood and *in vivo* in rats. *Biochemistry* **31**, 9141-9149.
35. Perutz, M.F. (1997). *Science is Not a Quiet Life. Unravelling the Atomic Mechanism of Hemoglobin*. pp. 473-500, World Scientific Publishing, London & Singapore.
36. Tsitsanou, K.E., *et al.*, & Fleet, G.W.J. (1999). The effect of most commonly used cryoprotectants on glycogen phosphorylase activity and structure. *Protein Sci.* **8**, 741-749.
37. Otwinowski, Z. (1993). Oscillation data reduction program. In *Proceedings of the CCP4 Study Weekend: Data Collection and Processing.* SERC Laboratory , Daresbury, Warrington, UK.
38. Brünger, A.T. (1996). *X-PLOR: Version 3.8; a System for Protein Crystallography and NMR*. Yale University Press, Newhaven, CT.
39. Martin, J.L., Withers, S.G. & Johnson, L.N. (1990). Comparison of the binding of glucose and glucose-1-phosphate derivatives to T state glycogen phosphorylase b. *Biochemistry* **29**, 10745-10757.
40. Read, R.J. (1986). Improved coefficients for map calculation using partial structures with errors. *Acta Crystallogr. A* **42**, 140-149.
41. *SYBYL Molecular Modelling Software*. (1992). Tripos Associates Inc., T.A. St Louis.
42. Jones, T.A., Zou, J.Y., Cowan, S.W. & Kjeldgaard, M. (1991). Improved method for building models in electron density maps and the location of errors in these models. *Acta Crystallogr. A* **47**, 110-119.
43. Luzatti, V. (1952). Traitment statistique des erreurs dans la determination des structur crystallines. *Acta Crystallogr.* **5**, 802-810.
44. Laskowski, R.A., MacArthur, M.W., Moss, D.S. & Thornton, J.M. (1993). PROCHECK: a programme to check the stereochemical quality of protein structures. *J. Appl. Crystallogr.* **26**, 283-291.
45. Kleywegt, G.J. & Jones, T.A. (1993). Biomacromolecular speleology. *ESF/CCP4 Newsletter* **29**, 26-28.
46. Hubbard, S.J. & Thornton, J.M. (1993). *NACCESS*, computer program. Department of Biochemistry and Molecular Biology, University College London.
47. Collaborative Computational Project Number 4. (1994). The CCP4 suite: programmes for protein crystallography. *Acta Crystallogr. D* **50**, 760-763.